

# Interatomic potential parameters for potassium tetrachlorozincate and their application to modelling its phase transformations

E. S. Ferrari,<sup>a</sup> K. J. Roberts,<sup>a†</sup> G. B. Thomson,<sup>a\*‡</sup> J. D. Gale<sup>b</sup> and C. R. A. Catlow<sup>c</sup>

<sup>a</sup>Centre for Molecular and Interface Engineering, Department of Mechanical and Chemical Engineering, Heriot-Watt University, Riccarton, Edinburgh EH14 4AS, Scotland, <sup>b</sup>Department of Chemistry, Imperial College of Science, Technology and Medicine, London SW7 2AY, England, and <sup>c</sup>Royal Institution of Great Britain, 21 Albemarle Street, London W1X 4BS, England. Correspondence e-mail: g.b.thomson@hw.ac.uk

An empirical fitting procedure is applied to derive interatomic potential parameters for a model phase transition system, namely potassium tetrachlorozincate ( $K_2ZnCl_4$ ). The derived potential is found to reliably model the known crystallographic structure for the ferroelectric and paraelectric phases of this compound. Potential transferability is demonstrated by applying the parameters derived to the optimization of the known molecular structure for a similar inorganic system (rubidium tetrachlorozincate).

© 2001 International Union of Crystallography  
Printed in Great Britain – all rights reserved

## 1. Introduction

The study of structural phase transitions in single crystals has always been of great interest as phase transformations often result in changes in crystal properties. One of the more topical types of phase transition are those involving ‘modulated crystal structures’, *i.e.* crystal structures that present any periodic, or partially periodic, perturbation with a repetition distance appreciably greater than the basic unit-cell dimensions (Cowley *et al.*, 1979). Such a perturbation can be described by a ‘modulation parameter’ ( $\gamma$ ), defined as the ratio of the component of the modulation wavevector ( $\mathbf{q}$ ) to the corresponding reciprocal-lattice basic vector (Hogervorst, 1986), *i.e.*

$$\mathbf{q} = \gamma \mathbf{a}, \quad (1)$$

where  $\mathbf{a}$  is the crystal lattice parameter along the modulation direction. If  $\gamma$  is rational then the structure is said to be commensurate, if  $\gamma$  is irrational the structure is referred to as incommensurate (Hogervorst, 1986). Phase transitions for this type of structure often involve transformation to or from a low-symmetry phase, exhibiting a pseudo-symmetry element, from or to a high-symmetry phase, where this pseudo-symmetry becomes a real symmetry element of the structure. Such slight deviations often produce polar structures and give rise to interesting physical properties, such as ferroelectricity, piezoelectricity, second-harmonic generation *etc.* Because the magnitude of non-linear properties often becomes enhanced close to the transition point, an improved understanding of the

inter-relationship between structural change and resultant physical properties allows, in principle, the engineering of material properties towards a desired outcome.

Molecular and solid-state modelling techniques use the simulation of the forces interacting between atoms and molecules by their mathematical description and, hence, allow the determination of the atomic positions and physical crystal properties. This provides the possibility of studying how the structure of a crystal changes as a function of temperature, and thus enables the relationship of the latter to any correlative physical and chemical property. This investigation was directed towards an examination of the applicability of molecular and solid-state modelling to phase transitions in solids in general and potassium tetrachlorozincate in particular.

## 2. Phase transitions in potassium tetrachlorozincate

A family of compounds that exhibits the type of phase transition described above and that has been intensively studied is those materials that crystallize in the  $A_2BX_4$  ( $\beta$ - $K_2SO_4$ ) structure. One of the members of this structural group, potassium tetrachlorozincate ( $K_2ZnCl_4$ , KZC), was used in this study as a model system. KZC crystallizes with a polar orthorhombic structure  $Pna2_1$  (Mikhail & Peters, 1979). The structure, which is typical of many compounds of this type, is ferroelectric (Gesi, 1978) and commensurate with a modulation wavevector  $\mathbf{q} = \mathbf{a}/3$ . Phase transitions in this material have been investigated by several workers and well defined phase transitions are known to take place at temperatures close to 403 and 555 K. Above the lock-in transition at 403 K, the structure is incommensurately modulated along the pseudo-

† Present address: Centre for Particle and Colloid Engineering, Department of Chemical Engineering, University of Leeds, Woodhouse Lane, Leeds LS2 9JT, England.

‡ Previously Telfer.

hexagonal  $a$  axis with a wavevector  $\mathbf{q} = 1/3(1 - \delta)\mathbf{a}$ , where  $\delta$ , the deviation parameter, increases with temperature until *ca* 555 K where the structure transforms to a paraelectric phase with the space group  $Pnam$ . KZC is a particularly interesting material in that its well defined incommensurate phase has such a long period of temperature stability.

Measurements of the thermal expansion and ultrasonic propagation in KZC around ambient temperature have been investigated (El-Korashy *et al.*, 1988, 1996, 2001) and provide an insight into the incommensurate phase transition that occurs at 403 K. A comparison of the elastic constants obtained from this system and those reported for other  $A_2BX_4$  systems indicates that, whilst the values observed for KZC are significantly lower, their relative magnitudes are of the same order. The observed trends within this series reflect the balance of steric against electrostatic contributions to the interatomic potential. Whilst in most crystals the temperature coefficients of the elastic constants are usually fairly similar, in this system,  $C_{13}$  exhibits an abnormally high temperature sensitivity (Fig. 1). This observation is consistent with the idea that the incommensurate phase transition, which is of first order (Shiba & Ishibashi, 1978), is associated with the generation of rotational disorder within the  $ZnCl_4^{2-}$  anion stacks.

### 3. Potential derivation methodology

Potential derivation modelling techniques involve the description of the interactions acting between the chemical species forming the crystal structure using mathematical equations (interatomic potential) that are deduced from the macroscopic properties (observables) of the substance or *via* quantum-mechanical methods. The empirical derivation of the parameters, contained in any interatomic potential, consists of a fitting procedure that involves:

- (i) the initial guess of parameters (in a specified expression);
- (ii) the adjustment of these parameters and the atom charges (according to the known crystal properties, the structure and the strains in and on the lattice);
- (iii) finally the improvement of the initial model and test for minimum energy.

For the system chosen, the general utility lattice program (*GULP*) (Gale, 1996, 1997) was employed in order to derive the potential parameters and a classical approach based on the Born model was applied. This model postulates that the energy of a system can be separated into two components, namely the electrostatic term ( $E_C$ ), based on Coulomb's law, and a two-/three-body central force interatomic interaction term ( $\Phi_{ij}$ ,  $\Phi_{ijk}$ ). The format of this second term used in this work for KZC includes the following:

- (i) description of the intermolecular repulsive interactions between the tetrachlorozincate anions *via* the Buckingham (Buckingham & Corner, 1947) potential;
- (ii) interatomic interaction between the potassium cations and the tetrachlorozincate anions simulated using the Buckingham potential form;

- (iii) the tetrachlorozincate group was considered as a molecular species, following the example of similar potential derivation carried out for alkali sulfate and alkali chlorate, bromate and perchlorate salts (Allan *et al.*, 1993; Telfer, 1997), hence intramolecular interactions were also considered. For the latter, a Morse potential for the Zn–Cl interaction and a three-body harmonic interaction were employed. The mathematical expressions relative to the potential form applied are reported below:

Buckingham  $\Phi_{ij} = A \exp(-r/\rho) - Cr^{-6}$  (2)

Morse  $\Phi_{ij} = D_e \{ [1 - \exp[-a(r - r_0)]]^2 - 1 \}$  (3)

Three-body harmonic  $\Phi_{ijk} = \frac{1}{2} k_b (\theta - \theta_0)^2$  (4)

The derivation of the energy parameters was achieved using empirical fitting to the structure adopted by the potassium tetrachlorozincate salt (KZC) at room temperature (Mikhail & Peters, 1979) and the elastic constants reported in the literature (El-Korashy *et al.*, 1996). The potential derived was then applied to minimize the structures for the ferroelectric (room-temperature structure), the incommensurate (Quilinchini *et al.*, 1990) (403–555 K) and paraelectric (Quilinchini *et al.*, 1990) (high-temperature structure) forms. The minimization process carried out within *GULP* uses the NR/BFGS method (Murtagh & Sargent, 1970; Shanno, 1970; Broyden, 1970). In order to take the thermal expansion into account, the optimization procedure employed the Gibbs free-energy-minimization method (Gale, 1998) instead of the

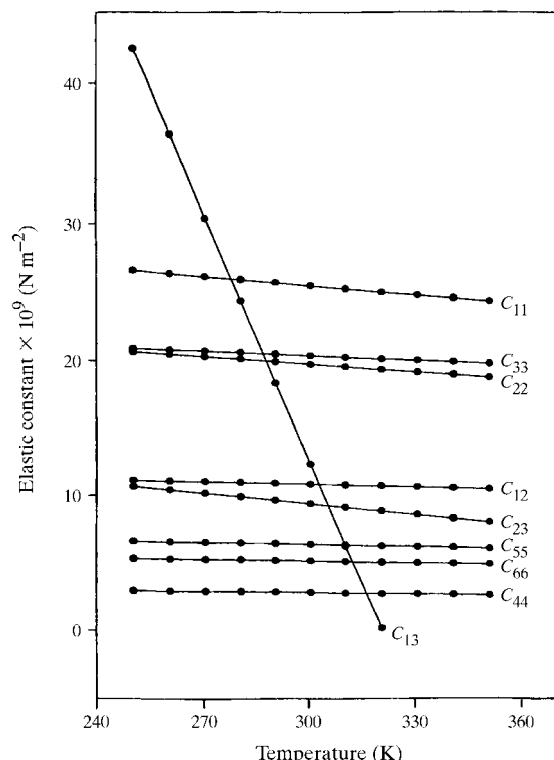


Figure 1 Variation of elastic constants with temperature for KZC single crystals.

**Table 1**

The potential parameters derived for KZC and RbZC.

Buckingham			
Interaction	$A$ (eV)	$\rho$ (Å)	$C$ (eV Å <sup>6</sup> )
K–Cl	6276.1323	0.290003	0.00000
Rb–Cl	4271.4845	0.295698	0.00000
Cl–Cl	0.0045120	0.254000	75.1600
Morse			
Interaction	$D_e$ (eV)	$a$ (Å <sup>-1</sup> )	$r_0$ (Å)
Zn–Cl	5.00000	0.53940	2.42298
Three-body harmonic			
Interaction	$k_b$ (eV rad <sup>-2</sup> )	$\theta_0$ (°)	
Cl–Zn–Cl	2.9388	109.500	

internal-energy method (*i.e.* vibrational and librational modes were considered). The cell parameters and atomic coordinates obtained were compared with those reported in the literature in order to assess the accuracy of the potential derived.

To test transferability, the potential parameters were also tested on the isomorphous compound rubidium tetrachlorozincate.

## 4. Results and discussion

### 4.1. Modelling the ferroelectric commensurate phase (*Pna2*<sub>1</sub>)

The refined interatomic potential parameters are summarized in Table 1 and the cell parameters for the different phases considered are reported in Table 2. The structure minimized (free energy equal to  $-426.96$  eV) at constant pressure for the paraelectric form was compared with that published by Mikhail & Peters (1979). A low percentage error between the lattice-parameter values determined by X-ray diffraction (Mikhail & Peters, 1979) and those calculated in the present work was found (1.72% for  $a$ , 1.28% for  $b$  and  $-0.28\%$  for  $c$ ). The structure derived by X-ray diffraction was compared with the simulated structure. Visualization, using the Cerius<sup>2</sup> molecular modelling software (Simulations Inc., Burlington, MA, USA, and Cambridge, England), along the three crystal axes revealed a slight rotation of the  $\text{ZnCl}_4^{2-}$  groups around the central zinc atoms following the structural optimization (viewed along  $\mathbf{a}$  in Fig. 2). The fractional coordinates for this phase before and after the minimization are compared in Table 3 and the potassium–chlorine and zinc–chlorine distances are summarized in Table 4. In Table 5, the elastic constant tensors are reported and compared with the experimental values. The predicted static dielectric constant tensors are reported in Table 6.

### 4.2. Modelling the paraelectric non-modulated phase (*Pnam*)

For the structure of the paraelectric phase, the data reported by Quilinchini *et al.* (1990) were considered. This

**Table 2**

Experimental and calculated lattice parameters for the ferroelectric, paraelectric and incommensurate phases of KZC.

Phase	Space group	Experimental lattice parameters (Å)	Calculated lattice parameters (Å)
Ferroelectric	<i>Pna2</i> <sub>1</sub>	$a = 26.789$ $b = 12.418$ $c = 7.259$	$a = 27.251$ $b = 12.578$ $c = 7.239$
Paraelectric	<i>Pnam</i>	$a = 8.960$ $b = 12.54$ $c = 7.300$	$a = 9.046$ $b = 12.579$ $c = 6.882$
Incommensurate	<i>Pnam</i>	$a = 8.960$ $b = 12.54$ $c = 7.300$	$a = 9.046$ $b = 12.578$ $c = 6.881$
Incommensurate	<i>Pna2</i> <sub>1</sub>	$a = 8.960$ $b = 12.54$ $c = 7.300$	$a = 9.147$ $b = 12.717$ $c = 7.322$

work proposed two different models for the description of this phase. In the first model, the structure is described using *Pnam* space-group symmetry. For the second model, a ‘split-atom’ description for the chlorine atoms was adopted in order to simulate their large thermal amplitudes (*i.e.* each chlorine atom was split into two different atomic types, Cl1 and Cl2). *Pnam* symmetry was also attributed to the ‘split-atom’ model. Only the ‘non-split’-atom model was considered for the structural minimization of the incommensurate phase using the derived potential. This is because the ‘split-atom’ model would imply a new fitting process that was not consistent with the central objective of this work, *i.e.* the derivation of a single force field with the ability to represent all the KZC phases.

The published data referred to a temperature of 588 K. The free-energy-minimization calculations for this structure gave rise to imaginary modes in the phonon spectra, hence a conventional optimization was carried out at constant pressure. Interestingly, Quilinchini *et al.* (1990) considered the same cell parameters for the incommensurate and normal phases in their study.

*‘Non-split’ Pnam model:* The cell parameters calculated for this structure agreed well with those used by Quilinchini *et al.* (1990) for the  $a$  and  $b$  axes, with the error to the experimental value being found to be  $<1\%$  (0.95 and 0.31%, respectively). For the  $c$  parameter, this error increased to 5.7% (Table 2). Together with the expected translation of the anionic group along the three crystallographic axis, some degree of rotation was also revealed (Fig. 3) following comparison with the reported structure. The centre of the rotation was found to lie in the middle of one of the Zn–Cl bonds. The fractional coordinates and interatomic distances for this structure, before and after minimization, are reported in Table 3 and Table 7, respectively.

### 4.3. Modelling the incommensurate phase (403–555 K)

As a reference structure for this phase, the one reported by Quilinchini *et al.* (1990) was also considered. For the description of the incommensurate structure, they used three models, namely the ‘non-split’-atom and the ‘split-atom’

**Table 3**

Fractional coordinates for the ferroelectric and paraelectric phase ('non-split'-atom *Pnam* model) of KZC before and after minimization.

Ferroelectric							
No.	Atom	Before minimization			After minimization		
		<i>x</i>	<i>y</i>	<i>z</i>	<i>x</i>	<i>y</i>	<i>z</i>
1	K1	0.0433	0.0814	0.7866	0.0452	0.0876	0.7866
2	K2	0.3797	0.0855	0.7638	0.3819	0.0874	0.7646
3	Zn1	0.0721	0.4194	0.7500	0.0734	0.4228	0.7498
4	Cl1	0.9917	0.4437	0.6731	0.9931	0.4452	0.6707
5	Cl2	0.1123	0.5756	0.8151	0.1125	0.5796	0.8148
6	Cl3	0.0844	0.3012	0.9795	0.0851	0.3014	0.9791
7	Cl4	0.1111	0.3560	0.4910	0.1121	0.3608	0.4930
8	K3	0.7106	0.0833	0.7223	0.7128	0.0825	0.7296
9	K4	0.3319	0.6875	0.7219	0.3321	0.6914	0.7284
10	Zn2	0.4050	0.4181	0.7796	0.4071	0.4208	0.7751
11	Cl5	0.3229	0.4366	0.8129	0.3249	0.4396	0.8150
12	Cl6	0.4439	0.5782	0.8132	0.4475	0.5760	0.8332
13	Cl7	0.4353	0.3072	0.9996	0.4355	0.2989	0.9771
14	Cl8	0.4306	0.3480	0.5110	0.4300	0.3637	0.4909
15	K5	0.6660	0.6863	0.7388	0.6661	0.6849	0.7403
16	K6	0.9986	0.6883	0.7932	0.9996	0.6906	0.7896
17	Zn3	0.7403	0.4177	0.7365	0.7415	0.4162	0.7441
18	Cl9	0.6591	0.4358	0.8044	0.6605	0.4328	0.8180
19	Cl10	0.7794	0.5760	0.6660	0.7787	0.5746	0.6741
20	Cl11	0.7778	0.3615	0.0026	0.7802	0.3617	0.0040
21	Cl12	0.7560	0.2942	0.5177	0.7560	0.2915	0.5221

Paraelectric

No.	Atom	Before minimization			After minimization		
		<i>x</i>	<i>y</i>	<i>z</i>	<i>x</i>	<i>y</i>	<i>z</i>
1	K1	0.6355	0.4114	0.7500	0.6303	0.4173	0.7500
2	K2	0.4942	0.8129	0.7500	0.4824	0.8178	0.7500
3	Zn3	0.2195	0.4205	0.7500	0.2273	0.4265	0.7500
4	Cl4	-0.0232	0.4288	0.7500	-0.0228	0.4203	0.7500
5	Cl5	0.3231	0.5797	0.7500	0.3166	0.5927	0.7500
6	Cl6	0.3063	0.3368	0.9945	0.3263	0.3495	1.0113

(which again was not considered in this work) models, described above, and a 'non-split'-atom model with polar space group *Pna2*<sub>1</sub>.

The data reported for this structure in the previous work (Quilinchini *et al.*, 1990) and in this work refer to the temperature of 453 K. For the 'non-split' *Pnam* model, the free-energy-minimization results showed again imaginary modes in the phonon spectra. For this model, an internal energy-optimization procedure was applied whereas, for the 'non-split' *Pna2*<sub>1</sub> model, the free-energy minimization was used. All the minimization procedures were carried out at constant pressure.

(a) '*Non-split*' *Pnam* model: The percentage error relative to the literature values for the cell parameters found after optimization were close to those determined for the paraelectric phase (*i.e.* 0.96% for the *a* axis, 0.3% for the *b* axis and 5.7% for the *c* axis; see Table 2). The analysis of the projections along the three crystallographic axes of the structure reported in the literature and the one obtained after minimization revealed that, together with the expected atomic translation along the three axes, a rotation of the tetrachlorozincate groups had occurred. The centre of this rotation seemed to lie on the mid-point of the Zn–Cl bond.

**Table 4**

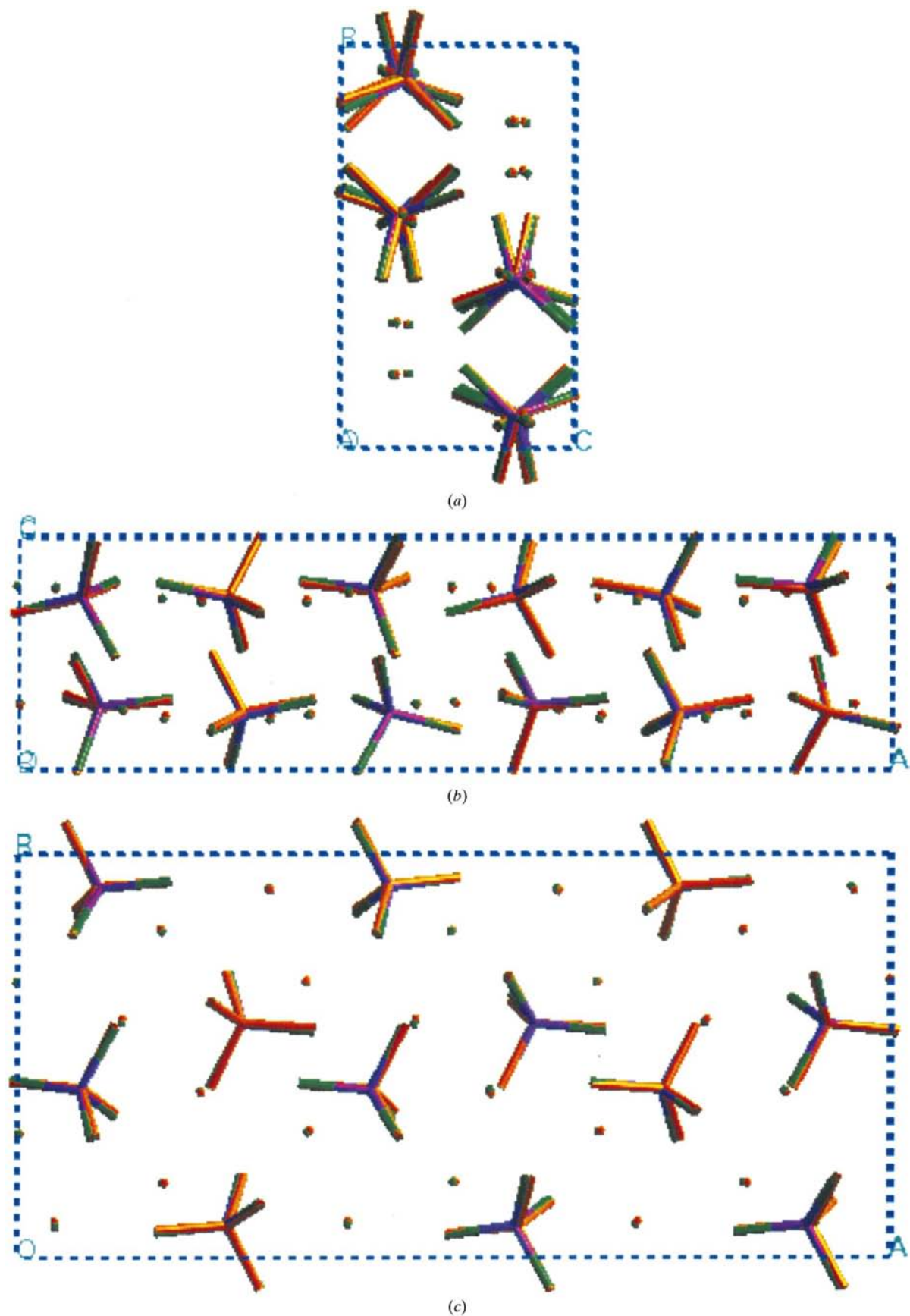
Comparison of metal–chlorine distances and chlorine–zinc bond lengths for KZC in the ferroelectric phase before and after minimization.

Before minimization		After minimization	
K–Cl distance (Å)	Zn–Cl bond length (Å)	K–Cl distance (Å)	Zn–Cl bond length (Å)
3.111	2 × 2.224	3.128	2 × 2.262
3.256	2 × 2.255	3.221	2 × 2.267
3.323	2 × 2.242	3.260	2 × 2.263
3.394	2 × 2.258	3.249	2 × 2.276
3.452		3.397	
3.558		3.431	
3.092	2 × 2.224	3.108	2 × 2.262
3.265	2 × 2.255	3.257	2 × 2.267
3.298	2 × 2.242	3.299	2 × 2.263
3.298	2 × 2.258	3.307	2 × 2.276
3.425		3.388	
3.564		3.490	
3.088	2 × 2.224	3.106	2 × 2.244
3.194	2 × 2.255	3.217	2 × 2.254
3.232	2 × 2.242	3.229	2 × 2.254
3.238	2 × 2.258	3.250	2 × 2.265
3.244		3.255	
3.357		3.442	
3.179	2 × 2.224	3.185	2 × 2.244
3.190	2 × 2.255	3.218	2 × 2.254
3.194	2 × 2.242	3.223	2 × 2.254
3.242	2 × 2.258	3.235	2 × 2.265
3.278		3.266	
3.357		3.393	
3.396		3.396	
3.402		3.430	
3.148	2 × 2.241	3.155	2 × 2.251
3.150	2 × 2.283	3.205	2 × 2.264
3.201	2 × 2.246	3.206	2 × 2.262
3.184	2 × 2.285	3.222	2 × 2.276
3.216		3.270	
3.248		3.337	
3.315		3.348	
3.354		3.449	
3.138	2 × 2.241	3.151	2 × 2.251
3.162	2 × 2.283	3.188	2 × 2.264
3.165	2 × 2.246	3.223	2 × 2.262
3.184	2 × 2.285	3.226	2 × 2.276
3.217		3.234	
3.249		3.244	
3.315		3.332	
3.354		3.345	

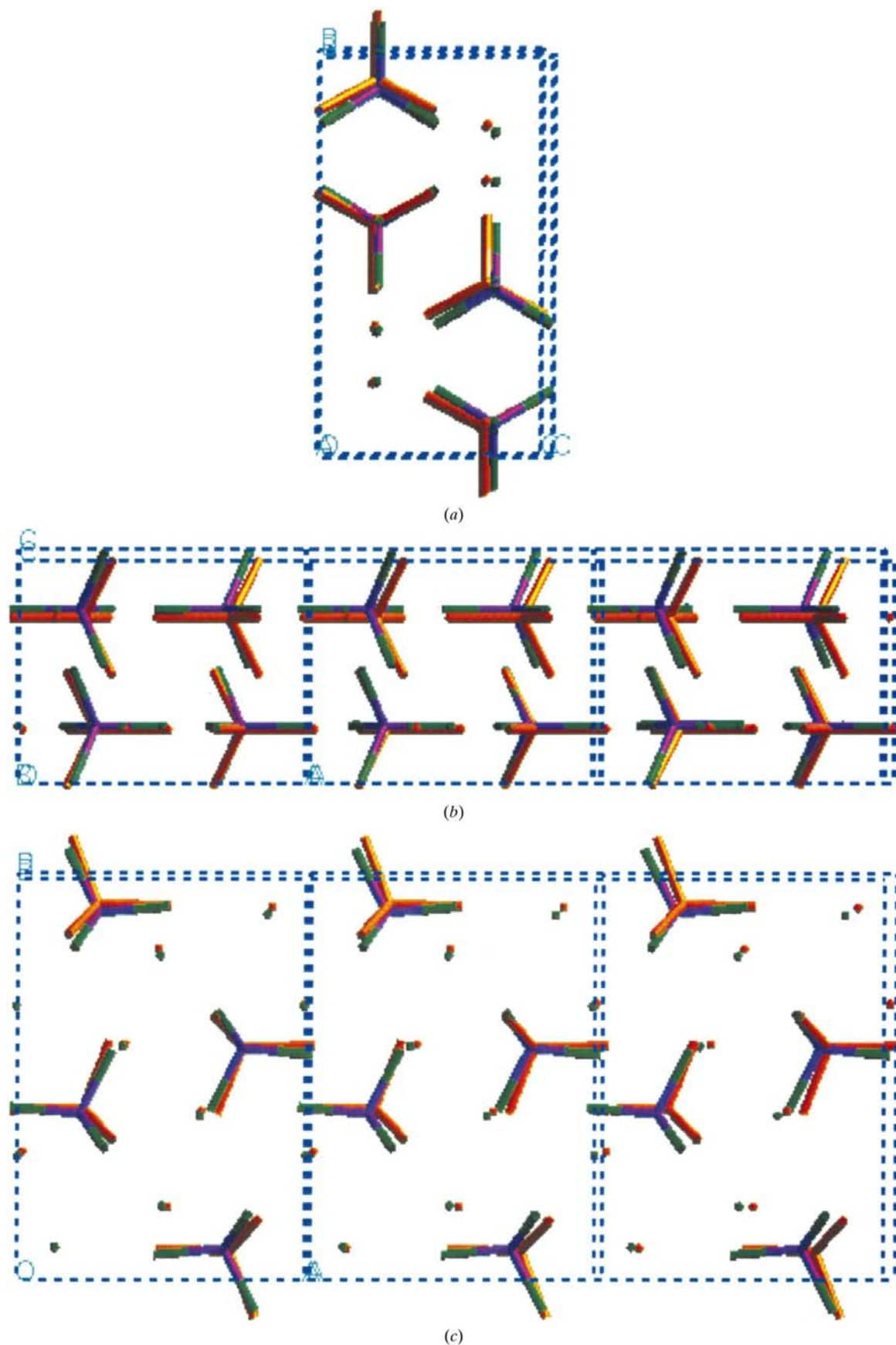
(b) '*Non-split*' *Pna2*<sub>1</sub> model: For this structure (free energy equal to -144.31 eV), the error with respect to the experimental value for the cell parameter along the *c* axis was found to be less than 1% (0.3%). The percentage errors calculated for the *a* and *b* parameters were found to be higher with respect to those determined for the *Pnam* model. From the comparison of the calculated structure with that reported by Quilinchini *et al.* (1990), it was possible to establish that the minimization of this geometry produced two types of rotation of the ZnCl<sub>4</sub><sup>2-</sup> groups; namely a rotation around one of the zinc chloride bonds and a rotation for which the centre was on one of the Cl atoms.

#### 4.4. Transferability of the derived potential

The possibility of transferring the potential derived for KZC to other similar systems was also investigated. Between the various structures belonging to the A<sub>2</sub>ZnCl<sub>4</sub> family, the



**Figure 2**  
Comparison of the experimental (multicolour) and calculated (orange) structures for the ferroelectric phase: (a) view along **a**, (b) view along **b** and (c) view along **c**.

**Figure 3**

Comparison of the experimental (multicolour) and calculated (orange) structures for the paraelectric phase: (a) view along **a**, (b) view along **b** and (c) view along **c**.

**Table 5**

The experimental and calculated values for the elastic constants ( $10^{10}$  Pa) for the different phases and models.

	Experimental ( $T = 298$ K)	$T = 298$ K ( $Pna2_1$ )	$T = 453$ K ( $Pna2_1$ )	$T = 453$ K ( $Pnam$ )	$T = 588$ K ( $Pnam$ )
C11	2.561	2.057	1.752	2.426	2.670
C22	1.982	1.882	1.156	1.769	1.603
C33	2.038	1.338	1.708	1.449	1.464
C44	0.280	0.517	0.525	1.000	0.980
C55	0.637	0.580	0.583	-1.871	39.859
C66	0.514	0.660	0.522	0.809	0.809
C12	1.079	0.430	0.195	0.453	0.476
C13	0.809	0.376	0.326	0.521	0.548
C23	0.918	0.659	0.536	0.211	0.210

**Table 6**

The predicted static dielectric constant tensors for the different phases and models.

	$T = 298$ K ( $Pna2_1$ )	$T = 453$ K ( $Pna2_1$ )	$T = 453$ K ( $Pnam$ )	$T = 588$ K ( $Pnam$ )
$xx$	2.897	3.213	2.695	2.735
$yy$	3.219	4.125	296.965	-47.942
$zz$	3.940	3.260	-10.422	-2.123
$xy$	0.000	0.000	-0.00001	-0.00001
$xz$	0.000	0.000	0.00006	
$yz$	0.000	0.000	0.00003	

inorganic salt  $Rb_2ZnCl_4$  (RbZC) was chosen in order to assess the transferability of the derived force field. In this the parameters relative to the two-body Cl-Cl interactions and the two- and three-body interactions for the tetrachlorozincate anion were all kept constant, whereas the alkali-Cl interaction was fitted considering the structural data reported in the literature for the ferroelectric phase. These new parameters (Table 1) were used to minimize the structures of the ferroelectric and paraelectric phases. The results obtained were compared with the data reported in the literature (Lu & Hardy, 1992) relative to each of the two structures.

The RbZC salt also crystallizes in the  $Pna2_1$  space group at room temperature (Lu & Hardy, 1992). The comparison with the experimental structure revealed that in the simulated compound the unit-cell parameters along the  $a$  and  $c$  axes were shorter with respect to the experimental values. The percentage error was found to be 0.29 and 1.65%, respectively (Table 8). On the other hand, the  $b$  parameter was found to increase owing to the minimization by 0.69%. The visualization of both structures showed that atomic translations along the three crystallographic axes took place after the optimization.

The second structure minimized for the rubidium salt belonged to the space group  $Pnam$  (Lu & Hardy, 1992) with the relative cell parameters being given in Table 4. For this configuration, it was found that the unit-cell length along the  $a$  axis increased after the optimization (the percentage error was 0.91%), whereas the  $b$  and  $c$  parameters decreased by 0.36 and 4.79%, respectively. Comparison of experimental and calcu-

**Table 7**

Comparison of metal-chlorine distances and chlorine-zinc bond lengths for KZC in the paraelectric ('non-split'-atom  $Pnam$  model) phase before and after minimization.

Before minimization		After minimization	
K-Cl distance (Å)	Zn-Cl bond length (Å)	K-Cl distance (Å)	Zn-Cl bond length (Å)
3.066	$2 \times 2.177$	3.138	$4 \times 2.230$
3.506	$4 \times 2.212$	$2 \times 3.385$	$2 \times 2.264$
$2 \times 3.572$	$2 \times 2.202$	$2 \times 3.395$	$2 \times 2.242$
		$2 \times 3.476$	
		3.595	
$2 \times 3.193$	$2 \times 2.177$	$2 \times 3.182$	$4 \times 2.230$
3.240	$4 \times 2.212$	3.204	$2 \times 2.264$
3.243	$2 \times 2.202$	3.226	$2 \times 2.242$
$2 \times 3.289$		$2 \times 3.264$	
3.302		3.294	

lated structures revealed that atomic translations had occurred following minimization with the potential derived.

## 5. Conclusions

The potential derived for the KZC salt using an empirical fitting routine gave satisfactory results when applied to the minimization procedure of the room- and high-temperature structures.

The transferability of the potential derived in this work was assessed *via* the minimization of the two structures of  $Rb_2ZnCl_4$ . The results showed a pleasing conformity with the data reported in the literature. The possibility of a free-energy minimization of the system is currently under investigation.

## 6. List of symbols

$\mathbf{q}$	modulation wavevector
$a$	crystal lattice parameter
$\gamma$	modulation parameter
$\delta$	deviation parameter
$\Phi_{ij}$	two-body interaction
$\Phi_{ijk}$	three-body interaction
$E_c$	electrostatic term
$A \rho C$	potential parameters for Buckingham potential
$r$	separation distance
$D_e$	depth of potential energy minimum
$a$	$(\mu/2D_e)^{1/2}\omega$
$\mu$	reduced mass of molecule
$\omega$	frequency
$r_0$	equilibrium bond length
$k_b$	bond-bending force constant
$\Theta$	coordinate angle
$\Theta_0$	equilibrium coordinate angle

The authors would like to thank A. El-Korashy (Oman College of Education), H. Klapper (University of Bonn) and R. A. Pethrick (University of Strathclyde) who were involved in the experimental work which formed the basis of this study. Interest in simulating molecular ionic systems has been

**Table 8**

Experimental and calculated lattice parameters for the ferroelectric and paraelectric phases of RbZC.

Phase	Space group	Experimental lattice parameters (Å)	Calculated lattice parameters (Å)
Ferroelectric	<i>Pna2<sub>1</sub></i>	<i>a</i> = 26.497	<i>a</i> = 26.421
		<i>b</i> = 12.188	<i>b</i> = 12.272
		<i>c</i> = 7.2250	<i>c</i> = 7.1060
Paraelectric	<i>Pnam</i>	<i>a</i> = 8.8080	<i>a</i> = 8.8880
		<i>b</i> = 12.492	<i>b</i> = 12.447
		<i>c</i> = 7.0970	<i>c</i> = 6.7570

stimulated *via* a long-standing collaboration with R. A. Jackson (University of Keele) who we also gratefully acknowledge.

## References

- Allan, N. L., Rohl, A. L., Gay, D. H., Catlow, C. R. A., Davey, R. J. & Mackrodt, W. C. (1993). *Faraday Discuss.* **95**, 273–280.
- Broyden, C. G. (1970). *J. Inst. Math. Appl.* **6**, 222–231.
- Buckingham, R. & Corner, J. (1947). *Proc. R. Soc. London*, **189**, 118–129.
- Cowley, J. M., Cohen, J. B., Salamon, M. B. & Wuensch, B. J. (1979). *Modulated Structures. AIP Conference Proceedings*, Vol. 53.
- El-Korashy, A. (1988). PhD thesis, University of Assiut, Egypt.
- El-Korashy, A., Gilmour, S., Pethrick, R. A. & Roberts, K. J. (1996). *J. Appl. Cryst.* **29**, 700–706.
- El-Korashy, H., Klapper, H., Pethrick, R. A. & Roberts, K. J. (2001). To be submitted to *J. Appl. Cryst.*
- Gale, J. D. (1996). *Philos. Mag.* **73**, 3–19.
- Gale, J. D. (1997). *J. Chem. Soc. Faraday Trans.* **93**, 629–637.
- Gale, J. D. (1998). *J. Phys. Chem.* **B102**, 5423–5430.
- Gesi, K. (1978). *Phys. Soc. Jpn.*, **45**, 1431–1432.
- Hogervorst, A. C. R. (1986). PhD thesis, Technische Hogeschool, Delft, The Netherlands.
- Lu, H. M. & Hardy, J. R. (1992). *Phys. Rev. B*, **45**, 7609–7620.
- Mikhail, I. & Peters, K. (1979). *Acta Cryst.* **B35**, 1200–1201.
- Murtagh, B. A. & Sargent, R. W. H. (1970). *Computer J.* **13**, 185–194.
- Quilinchini, M., Bernede, P., Lefebvre, J. & Schweiss, P. (1990). *J. Phys. Condensed Matter*, **2**, 4543–4558.
- Shanno, R. F. (1970). *Math. Comput.* **24**, 647–656.
- Shiba, H. & Ishibashi, Y. (1978). *J. Phys. Soc. Jpn.*, **44**, 1592–1599.
- Telfer, G. B. (1997). PhD thesis, University of Strathclyde, Glasgow, Scotland.